Vol. 88 No. 6 pp. 1729–1741 ACTA GEOLOGICA SINICA (English Edition) Dec. 2014

Mica Inclusions inside Host Mica Grains from the Sutlej Section of the Higher Himalayan Crystallines, India—Morphology and Constrains in Genesis

Soumyajit MUKHERJEE*

Department of Earth Sciences, Indian Institute of Technology Bombay, Powai, Mumbai-400 076, Maharashtra, India

Abstract: Biotite and muscovite inclusions inside mica host minerals from the Sutlej section of the Higher Himalayan Crystalline were studied under an optical microscope. These inclusions formed possibly by local recrystallization of mica grains during regional prograde metamorphism, with some affected by top-to-SW shear leading to parallelogram shapes. Recrystallization may have been assisted by solution transfer along the cleavage planes of the host grains. The relative competency of deformed phyllosilicate inclusions with the same or different composition to the host depends on the size and orientation of (001) cleavage planes of the inclusions relative to the host. Shearing of mica inclusions led to their parallelogram geometries within the contained mica inclusions. Some of the sheared inclusions deflect cleavage planes in the host minerals and define flanking microstructures. Trapezoid-shaped inclusions are a new finding that deserves more attention for their genesis. These structurally anisotropic inclusions did not originate from sub-grains, secondary infillings or retrogression. These inclusions are also not related to pseudomorphism, isomorphism, folding of the bulk rock etc. Some of the inclusions formed by recrystallization of the host mineral during top-to-SW ductile shear.

Key words: nucleated mica grains, inclusions, shear zones, ductile shear, deformation, Himalaya

1 Introduction

Several qualitative and quantitative micro-structural investigations from the 1950s led to infer the kinematic implications of nucleated mineral grains inside host minerals (e.g. Wahlstrom, 1955; Heinrich, 1956; Kretz, 1966; Vernon, 1977; Bell, 1978; Vernon, 2004). Salient conclusions are: (i) Euhedral inclusions in igneous rocks formed before their host minerals (Heinrich, 1956). As a corollary, subhedral and anhedral inclusions crystallized presumably synchronously or after their host minerals. (ii) Secondary minerals may fill up sub-spherical micro-cavities of the host grains to form 'peg structures', which are relatively common in mellilites (Fig. 1a; drawn from fig. 4 of Wahlstrom, 1955). Obviously, such secondary minerals formed later than the host minerals. Secondary mineralization has also been suggested for neocrystallized micas in dilation zones (Vernon, 1977). Be it in mellilites or micas, such structures constitute linear sets of mineralization with lobate terminations (Wahlstrom, 1955). (iii) An inclusion structurally isotropic (not necessarily optically isotropic) with the host mineral should possess a rounded morphology (Kretz, 1966 and references therein). An isotropic inclusion on deformation is expected to become lenticular/elliptical, i.e. elongate along with rounded corners. (iv) The preferred orientation of inclusions within porphyroblasts with respect to the foliation pattern in the matrix is useful to deduce the time relation between deformation and the growth of such porphyroblasts (e.g. Bell and Hobbs, 2010). (v) The inclusion may inherit its form by imposition from the host mineral (Kretz, 1966). However, such pseudomorphism will be difficult to establish if the inclusion and the host mineral belong to the same species. (vi) Inclusions could also be the remnants of a prior (low-grade) metamorphism where a late stage mineral started developing at the margin of the former and left only a remnant of the latter (Vernon 2004). (vii) Inclusions and their host minerals must be chemically inert for a specific geological span; otherwise they would have reacted and altered (Vernon, 2004). (viii) Recrystallization inside micas can form smaller unstrained

* Corresponding author. E-mail: soumyajitm@gmail.com

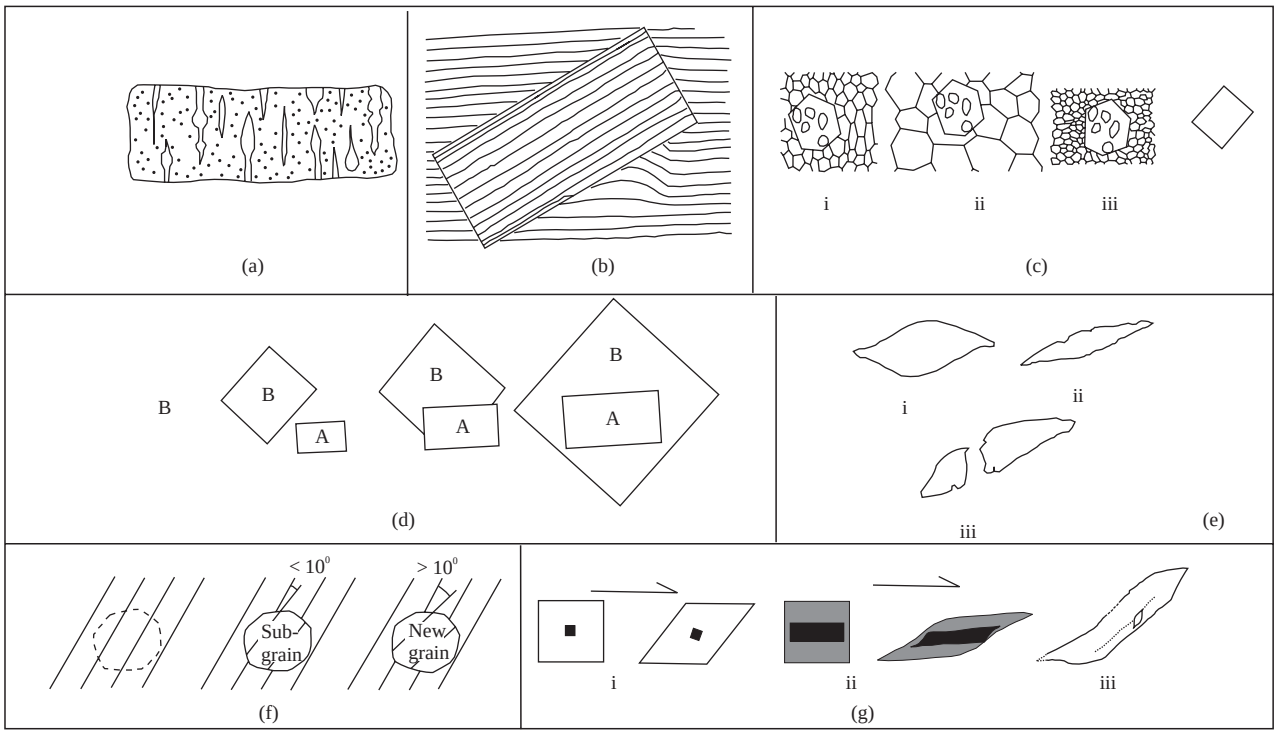

Fig. 1. Salient points on inclusions.

a. A greatly magnified peg structure (drawn from fig. 4 of Wahlstrom, 1955). b. Inclusion of a rectangular mica grain over kinked portion of a host mica mineral (drawn from fig. 5D of Bell 1978). (c. i) Inclusions inside a prophyroblast are nearly of same size to that of minerals of same species in the matrix. (c. ii) Inclusions smaller than the matrix minerals indicates that the matrix grains grew and underwent static recrystallization. (c. iii) Inclusions larger than the matrix grains indicate that the matrix underwent dynamic recrystallization (drawn from fig. 7.27 of Passchier and Trouw, 2005). d. Mineral 'A' started growing later and slower than the mineral 'B' and eventually 'A' occurs as an inclusion inside 'B' (drawn from fig. 3.47 of Vernon, 2004). (e) Dissolution of sharp margins of mineral inclusions made them smooth (drawn from figs. 80A and –B: Simpson, 1998). (f) A subgrain after > 10° rotation occurs as an inclusion (drawn from fig. 10.18a of Fossen, 2010). (g) In simple shear, a square inclusion harder than the matrix undergoes more rotation than internal deformation; but (g. ii) a softer inclusion deforms preferentially into a parallelogram (drawn from fig. B.5.4. of Passchier and Trouw, 2005). (g. iii) Ductile sheared muscovite fish that also contains a smaller sigmoidal inclusion of biotite grain (outlined from fig. 12c of Mukherjee, 2011a).

inclusions of the same mineral species (Vernon, 1977). (ix) Undeformed new rectangular micas sometimes nucleate within kinked mica grains (Fig. 1b**;** Bell, 1978).

The following points summarize interpretation of inclusions in the light of kinematics. (i-a) Inclusions may be incorporated from the matrix by migration of the boundaries of what are now the host grains. Such inclusions are the type-1 varieties (Fig. 1c-i; Vernon, 2004) (i-b) By contrast, the type-2 inclusions grows coevally with the host (Vernon, 2004). (ii) A mineral that grows at a faster rate can incorporate an adjacent mineral grain from the matrix that grows at a slower rate (Fig. 1d; Vernon, 2004; Gill, 2010). Here the original angle between the inclusion and the external foliation remains constant. (iii) Inclusions with smooth margins might form by dissolution of their euhedral boundaries (figs. 80A and –B of Simpson, 1998; outline reproduced here in Fig. 1e). (iv) Micas can nucleate and grow in any preferential direction of chemical transport to produce inclusions oriented in a specific direction (Vernon, 1977). (v) Some inclusions form by moderate rotation (> 10°) of sub-grains (Fig. 1f; Fossen, 2010). These inclusions are characteristically rounded. (vi) When the bulk rock undergoes simple shear, inclusions weaker than the host minerals assume overall parallelogram shapes with a little sigmoidality, while stronger inclusions undergo rigid body rotation and perhaps with some ductile deformation (Fig. 1g; Passchier and Trouw, 2005). A sigmoid-like inclusion of mica (Fig. 1g-iii) has also been reported by Mukherjee (2011a) from a Himalayan shear zone where the former genesis might apply. (vii) If the bulk rock folds, the inclusions tend to elongate along the fold axis (Passchier and Trouw, 2005). However, depending on the strain ellipsoid, inclusions may also be oriented differently. Folded rock can be confirmed from field observations or in thin-sections from the folded external foliation (or the 'S-external') planes. (viii) While the occurrence of progressively smaller inclusions towards the rim of the host minerals connote a systematic variation in growth rate of the host mineral; the opposite scenario signals an elevation of temperature of the bulk rock (Vernon and Clarke, 2008). (ix) Mukherjee and Koyi (2009) report cases of dragged and slipped cleavage planes of host mica grains near inclusions of smaller micas as 'flanking

microstructures' from sheared rocks at a number of river sections of the northwestern Indian Higher Himalayan Crystalline. The shape asymmetry of the inclusion in these cases always represents the true ductile shear sense (also see Mukherjee, 2010a, b; Mukherjee and Koyi, 2010a, b; Mukherjee, 2011a, b).

This work describes mica inclusions inside mica host minerals from the Sutlej section of the Indian Higher Himalayan Crystallines, and selectively deciphers their kinematic implications. In particular, the conspicuous points on the morphology and genesis of the inclusions compiled in the previous paragraphs are also tested.

2 Geology of the Study Area

The Higher Himalayan Crystallines (HHC) in the Himalayan mountain chain is bound by the Main Central Thrust-Lower at south and the South Tibetan Detachment System in the north. The HHC in the Sutlej River section (Fig. 2) in the Kinnaur district of Himachal Pradesh (India) consists of gneisses and schists of Precambrian and Proterozoic ages at dominantly greenschist to amphibolite metamorphic facies (Grasemann et al., 1999; Vannay et al., 1999; Vannay and Grasemann, 2001). The Munsiari Thrust skirts the underlying Lesser Himalayan Larji-Kulu-Rampur Window of metasedimentary rocks. Through the location Karcham passes the MCT-Upper (MCT_U; as followed by Mukherjee and Koyi, 2010a; Mukherjee, 2010a; Mukherjee, 2013a, b). Chambers et al. (2009) considered it as the 'true' Main Central Thrust. The HHC might be a curvi-planar shear zone (Mukherjee and Biswas 2014). Jain et al. (2000) and Richards et al. (2005) briefly described the stratigraphy of the Sutlej section of the HHC. Extension of the Main Central Thrust and the South Tibetan Detachment along the Himalayan chain were described by Burchfiel et al. (1992), Carosi et al. (2008),

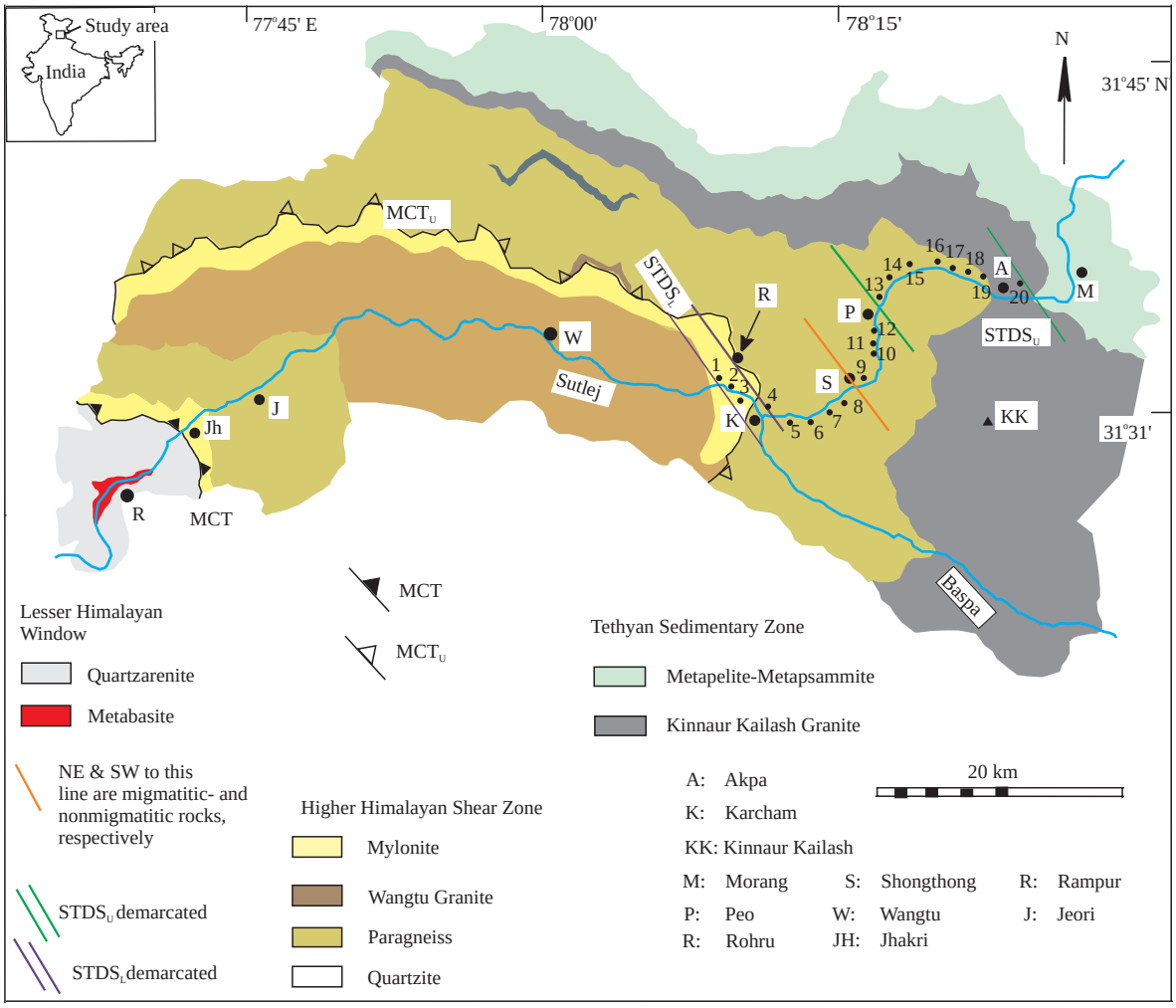

Fig. 2. Geological map of the Higher Himalayan Crystalline (compiled and simplified from S. Singh, unpub Ph.D. thesis, University of Roorkee, 1993; Srikantia and Bhargava 1998; and Vannay and Grasemann 1998). Srikantia and Bhargava's (1998) Vaikrita Thrust is denoted by Godin et al.'s (2006) 'MCT-Upper' (MCT_U). The two strands of extensional ductile shear zones- the BD and the STDS- are shown as per Mukherjee and Koyi (2009a). Numbers 1 to 20 represent sample locations.

Searle et al. (2008), Mukherjee (2013a, b) - to name a few. Rocks NE of the MCT_U belong to the Vaikrita Group (Srikantia and Bhargava, 1998). Mukherjee (2010a) presented a detailed photographic description of structures of this shear zone from field and microscopic studies (also see Mukherjee 2013c, d). Mukherjee (2007, 2010a) and Mukherjee and Koyi (2010a) grouped rocks from Karcham up to Shongthong in the NE along the river section as the 'non-migmatitic' and from Shongthong up to the northern extremity of the HHC as the 'migmatitic'. The thin-sections studied here come from both the migmatitic and the non-migmatitic rocks of the HHC that are NE to the MCT_U. This upper-part of the HHC underwent two dominant extrusion phases in the ductile regime (Mukherjee and Koyi, 2010a). During the E_1-phase of extrusion, a top-to-SW sense of ductile shearing happened during ~25-19 Ma along NE dipping foliation planes. The subsequent E_2-phase of extrusion from ~15 to 12 Ma involved a combination of simple shear at the boundaries of the HHC and an extrusive pressure gradient. These processes resulted in top-to-NE extensional ductile shear along the pre-existing NE dipping shear planes in both the South Tibetan Detachment System (STDS) and the Basal Detachment (BD). That the BD and the MCT_U nearly coincides has also been reported from other Himalayan sections by Janda et al. (2002), Takagi et al. (2003), Jain et al. (2012) and Mukherjee (2013a). Much south to Karcham, an out-of-sequence thrust passes through the location Chaura (Jain et al., 2000; Mukherjee et al., 2012). Finally, a top-to-SW sense of brittle shear occurred along the pre-existing ductile shear C-planes that dip NE. This occurred as a pre-12 Ma event (Mukherjee and Koyi, 2010a). In other words, the earlier ductile C-planes latter reactivated as the Y-planes of brittle shear. A component of pure shear has also been quantified in terms of a kinematic vorticity number of 0.86 (Grasemann et al., 1999) and 0.73-0.81 (Law et al., 2013). Chambers et al. (2011) postulated that both channel flow and critical taper mechanisms were active at different time periods in the Sutlej section of the HHC. They deciphered, based on U-Th-Pb dates of monazites, that channel flow started at ~25-20 Ma back, and each deformation mechanism lasted for ~2-5 Ma.

The three metamorphic episodes of the Sutlej section of the HHC are: (i) pre-Himalayan M_1 metamorphism that took place around granite plutons of 2.0 to 0.5 Ga; (ii) main-Himalayan prograde M_2 metamorphism characterized by the growth of porphyroblasts induced by crustal thickening during the top-to-S/SW ductile shear from ~25 Ma onwards (the D_2 deformation), and (iii) post-Himalayan M_3 metamorphism indicated by the development of chlorite and muscovite in place of biotite, garnet and staurolite (Jain et al., 2002 and references therein) during unroofing, with unknown timing (Yin, 2006). Based on recent published data, Guillot and Replumaz (2013) presented a different three-phase classification of metamorphism of the HHC. However, given that the stated broad time range of the M2 metamorphism incorporates a ~1.8 Ga event of plutonism in the Lesser Himalayan rocks and a ~500 Ma event in the HHC, such a vast time span of M2 remains debatable (as per Delores Robinson, personal communication). Northward from the MCT_U, the peak M_2 metamorphism is characterized by an increase in temperature from 570°C to 750° C at nearly a constant pressure of 8 MPa. The presence of isograds of higher-grade minerals at the base indicates an inverted metamorphism within the HHC (Vannay et al., 1999; Vannay and Grasemann, 2001). Tectonic evolution of Tibet (Dai et al. 2014; Wu et al. 2014) can be interpreted by studying structural geology of the Himalaya.

3 Mica Inclusions within Host Mica Grains

3.1. Morphology and deformation

The angle between one of the margins of the inclusions to the single set cleavage planes of the host mica grains varies from 24° to 75° (Figs. 3-7), while the other margin sub-parallels the cleavage planes. Thus, the two dominant directions of growth of mica inclusions are sub-parallel to the cleavage planes of the host, and the other at an angle to it. The finding is similar to that from a peraluminous granite body by Roycroft (1991). Following Kretz (1966), the semi-preferred orientation of inclusions indicates that they tried to minimize their interfacial energies. (The total free energy of molecules at the margin of the inclusions is its 'interfacial energy') These angles, however, do not indicate any simple estimate of shear strain because inclusions behave differently depending on whether or not they are stronger than the host mineral (see Passchier and Trouw, 2005 for a brief review). Even when the inclusion and the host mineral belong to the same mineral species, the inclusion acquires a parallelogram shape (Figs. 3d, 4b; 5a; 6a; 6b) due to ductile shear. Rectangular micas in thin-sections on shear are expected to become parallelogram-shaped (e.g. Mukherjee, 2011a). Similar observations of deformed micas inside hosts of the same mica species were also made by Mukherjee (2009, 2011a), Mukherjee and Koyi (2009), and Gill (2010) - to name a few. Even if no estimate of viscosity is available for most of the minerals including micas, the included mineral grain should have a viscosity slightly different from that of the host grain of the same mineral species. Had they were of same viscosity, they should have led to the same shape.

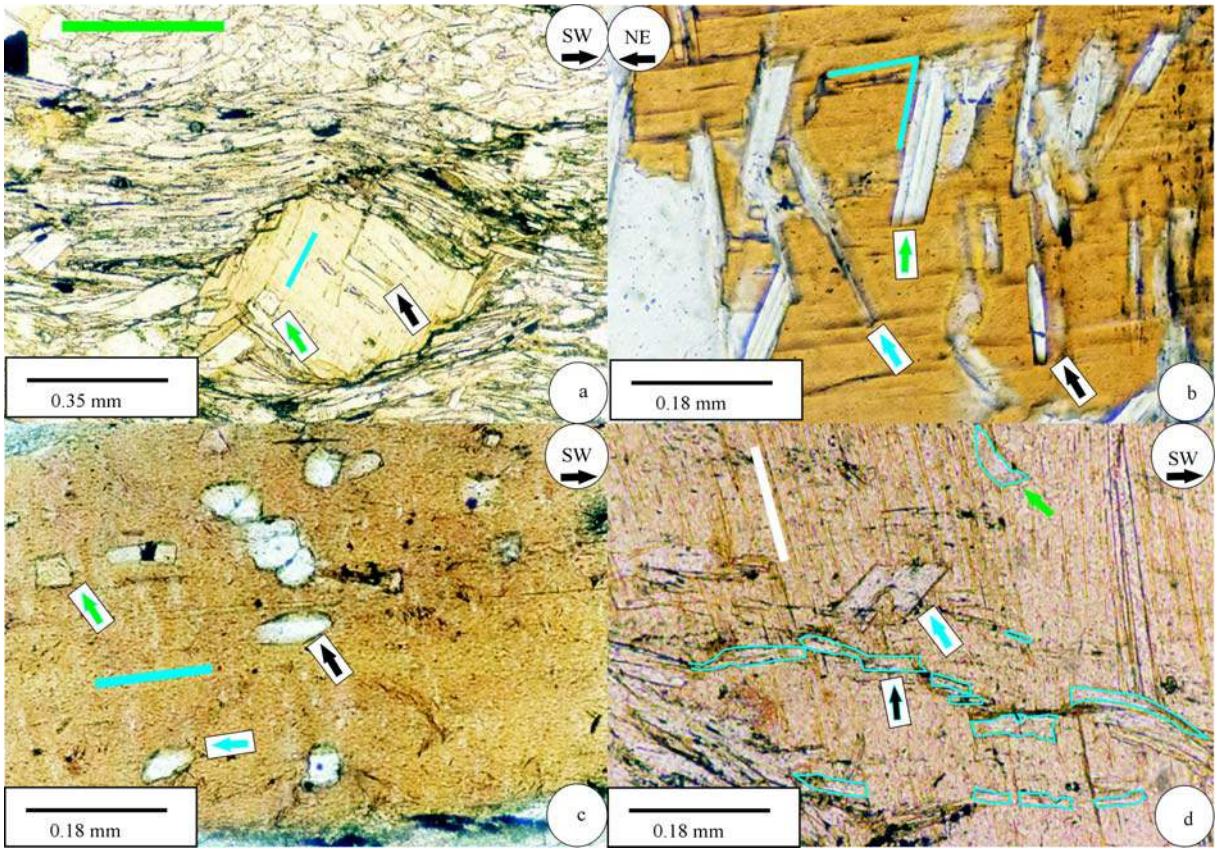

Fig. 3. All photos in plane polarized light.
(a), Sample: 3. A nearly symmetric lenticular single biotite fish with a number of inclusions of muscovite grains most of which (black arrow) are elongated at high angle to the cleavage planes (blue line) of the fish. Only a single inclusion is squarish (green arrow). The thick green line represents the nearly straight orientation of the main foliation. (b), Sample: 3. At a higher magnification and after rotation of the stage of the microscope, cleavage planes of the muscovite inclusions of Fig. 3a become visible. Those cleavage planes are also at a high angle (~75°) to that of the host grain. The acute angle is shown by two blue lines. The inclusions are parallelogram-shaped with one of their margins roughly parallel the cleavage planes of the host mineral. Some of the thicker inclusions are tilted top-to-right (green arrow), few thinner ones top-to-left (blue arrow), and yet other nearly orthogonal (black arrow). (c), Sample: 2. Whereas a single inclusion of biotite inside a biotite host mineral is square (green arrow), the quartz grains are either irregular (blue arrow), or elongated (black arrow) towards the cleavage planes of the host mineral. The other margin of the inclusion in the latter case is at high angle to the cleavage planes (e.g. at black, blue and green arrows). (d), Sample: 19. A parallelogram-shaped biotite inclusion (blue arrow) at an angle to the cleavage planes (white line) of the host biotite grain. Here none of the margins of the inclusions roughly parallel the cleavage planes of the host. Other smaller inclusions of biotites are mostly rectangular and parallelogram-shaped (black arrow), with one of their nearly straight margins roughly parallel the cleavage planes of the host mineral. Some of these inclusions seem to be interconnected with each other, and the others are not the trapezoid shaped inclusion of biotite (green arrow) is rare.

Biotite deform easier than muscovite (possibly because dissolution of the former is more dominant than the latter; Wilson and Bell, 1979). Shearing of inclusions of biotite in muscovite are comparable to that of weaker inclusions in a stronger matrix. In such cases, as per Passchier and Trouw (2005), simple shear would lead to parallelogram-shaped inclusions with rounded corners (Fig. 1g-ii. Similarly, non-coaxial shear of muscovite inclusions within biotite hosts is expected to rotate the internally undeformed muscovite grains to maintain high angles between their margins (or cleavage planes) (Fig. 1g-i). In this study, examples of both more competent inclusions inside weaker hosts: muscovite within biotite (Figs. 3a-c; 4a, -c, -d; 5c, -d; 6c, -d) and also biotite within muscovite (Fig. 5b) were encountered. The former types are more common.

In many cases, inclusions of deformed micas, muscovite and biotite, cut across the visible cleavage planes of their host micas. The host cleavage planes curves near the contacts with the inclusions. Curved host cleavage planes and the fact that these inclusions are most often parallelogram-shaped (Figs. 3b-d; 4a, -c, -d; 5a; 6b, -c) (cf. Mukherjee 2007; 2010a, b; 2011a; Mukherjee and Koyi 2009) indicate that those inclusions underwent ductile shear that led to drag (and possibly slip) on the cleavage planes of the host mineral in contact with them. These inclusions qualify as ‘cross-cutting elements’ (CEs) and the cleavage planes of the host minerals the ‘host fabric elements’ (HEs). The CE and HE together is called as ‘flanking structures’ (Passchier, 2001; Mukherjee and Koyi 2009). Mukherjee and Koyi (2009) showed that a pair of margins of such inclusions roughly parallels the

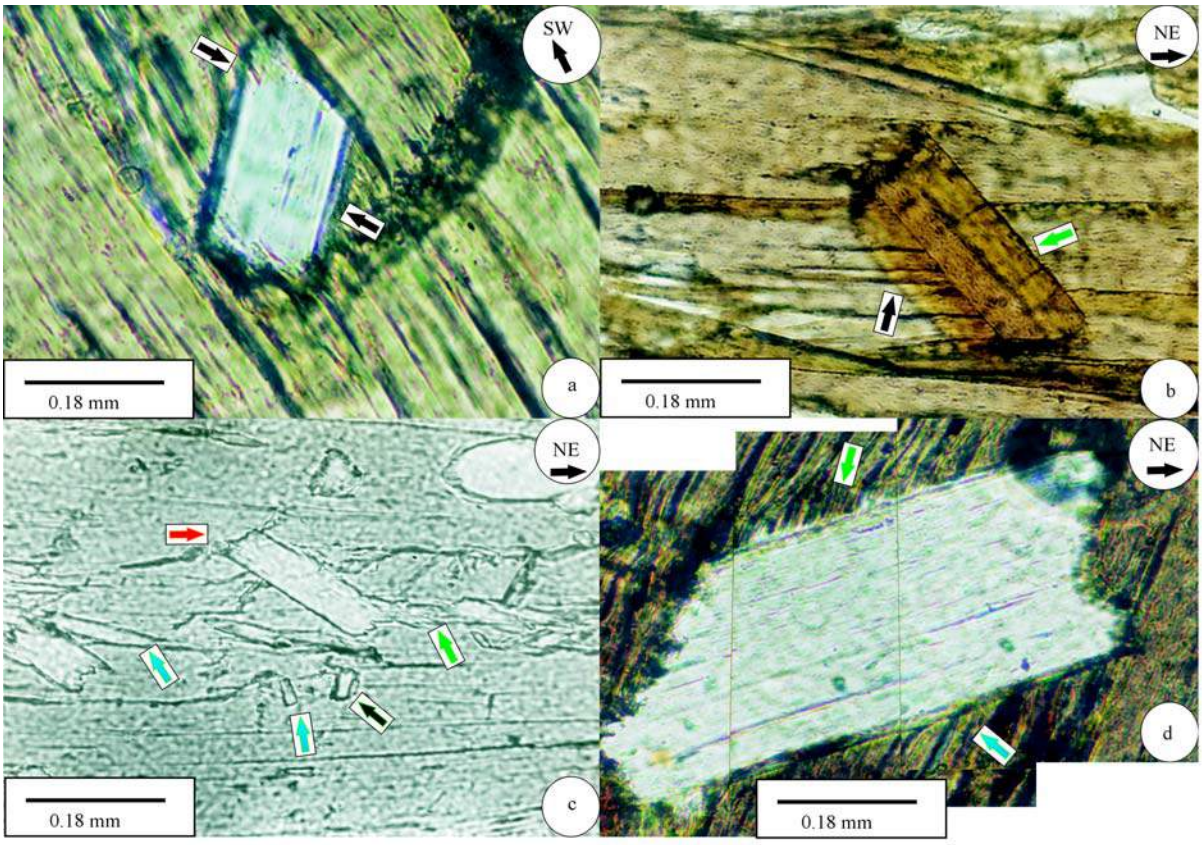

Fig. 4. All photos in plane polarized light.
(a), Sample: 7. A parallelogram-shaped muscovite inclusion with a biotite host shows drag of cleavage planes of the latter near the boundaries (arrows) of the former. A pair of margins of the inclusion is at a low-angle to the cleavage planes of the host, while the other pair is at ~45°. The inclined margins are diffuse, whereas the roughly parallel margins are not. Cleavage planes of the host grain penetrate the inclusion (arrow at left). Gentle drag of cleavage planes is noted; hence the cleavage planes and the nucleated grain together constitute a flanking structure. (b), Sample: 10. One of the margins of a biotite inclusion inside a biotite shows a thick hazy zone (black arrow), whereas the other side (green arrow) is sharp. A pair of margins of the inclusion roughly parallels the cleavage planes of the host, while the other pair is at ~52°. Near the former margin, the cleavage planes of the host are gently 'convex up' (blue arrow). (c), Sample: 20. A parallelogram-shaped inclusion of muscovite (orange arrow) inside a biotite host shows a top-to-left shear, which is also demonstrated by a much smaller muscovite inclusions (blue arrows). A pair of margins of the former inclusion roughly parallels the cleavage planes of the host, while the other pair is at ~33°.The former inclusion is associated with dissolution of material and precipitation along the cleavage planes of the host (green arrow). (d), Sample: 15. A flanking microstructure defined by a muscovite grain as the cross-cutting element and swerved cleavage planes of the biotite host grain as the host fabric element. A pair of margins of the inclusion roughly parallels the cleavage planes of the host, while the other pair is at ~40°.

cleavage planes of the host mineral, whereas the other pair of margins is non-parallel. Either single or both the margins of the inclusions are diffuse due to penetration of the cleavage planes at the inclusion margins. These observations were found to also apply to the studied flanking microstructures (Figs. 4a, -b, -d; 5a-c; 6a-c).

Trapezoid-shaped inclusions of micas are present (Figs. 7a-c) where none of the trapezoid margins roughly parallel the cleavage planes of the host mica grains. Trapezoid-shaped minerals in the matrix are described by Mukherjee (2008, 2010a, b) and Mukherjee and Koyi (2010a, 2010b) under optical microscopes. These trapezoids were interpreted as microscopic equivalent of thrust slices. However, thrust movement of trapezoid inclusions inside any host mineral seem implausible and requires further study.

3.2. Conjectured genesis

As the studied rocks are metamorphic, one cannot straightway comment on the relative timing of growth between the mica inclusions (Figs. 3-7) and their host micas based solely on the shapes of the inclusions. Isomorphism of one mica species into the other leading to the genesis of mica inclusion is also negated as no such reactions (Yardley, 1996) exist. As none of the studied mica inclusions are (sub)circular (Figs. 3-7), they are structurally anisotropic with the host mica grains. Both biotite and muscovite share the same sheet silicate structure. Therefore following Vernon and Clarke (2008), such a relation between the inclusion and the host mineral can be termed 'epitaxial'. Electron back scattered diffraction studies of some epitaxial minerals to unravel their genesis are available (e.g. Hammer et al., 2010), but none on micas. The fluid condition during metamorphism

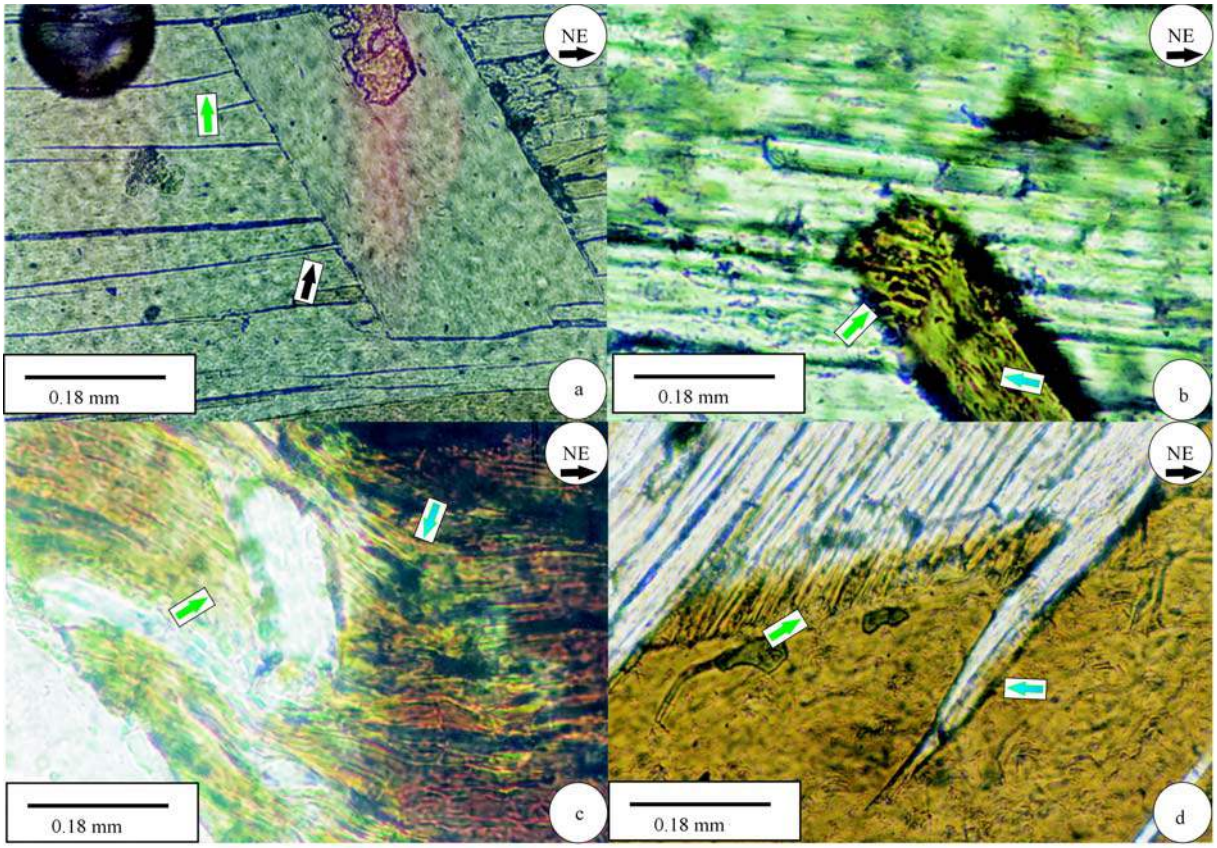

Fig. 5. All photos in plane polarized light. a-c. Flanking microstructures.
(a), Sample: 17. A muscovite included within a muscovite host grain. Parallelogram shape of the inclusion indicates a top-to-left shear. The cleavage planes of the host grain at the same side of the inclusion are variably concave up curved (arrows). The inclusion margins are very sharp. A pair of margins of the inclusion roughly parallels the cleavage planes of the host, while the other pair is at ~62°. (b), Sample: 14. A biotite inclusion inside a muscovite host was internally deformed as revealed by its warped cleavage planes (blue arrow). The cleavage planes of the host mineral strongly penetrate the inclusion and are convex up (green arrow). A pair of margins of the inclusion roughly parallels the cleavage planes of the host, while the other pair is at ~57°. (c), Sample: 18. An internally deformed muscovite grain reveals opposite senses of drag (convex up at green arrow and concave up at blue arrow) of the cleavage planes of the across it. A pair of margins of the inclusion roughly parallels the cleavage planes of the host, while the other pair is at ~40°. (d), Sample: 15. A biotite inclusion with muscovite shows digitations of the latter inside the former (blue arrow) and penetration and minute curvature of cleavage planes of the latter into the former (green arrow). The digitation is similar to that of hornblende inside the surrounding matrix in micro-scale as reported by Philpotts and Ague (2009). A pair of margins of the inclusion roughly parallels the cleavage planes of the host, while the other pair is at ~42°.

of the bulk rocks could be ascertained from inclusion of minerals using Laser Raman Spectrophotometry (e.g. Liu et al. 2001). Muscovite inclusions inside garnets have been studied to decipher the regional metamorphism (e.g. Faryad et al., 2010). Laser ablation Ar-Ar dating of biotite inclusions inside garnets were deduced by Kelley et al. (1997). Electron microprobe revealed five generations of monazite inclusions from garnet host minerals from the Langtang section of the HHC in Nepal (Kohn et al., 2005). But such works are beyond the scope of this study.

As inclusions arising from subgrains must be of the same mineral species as the host (Fossen, 2010), presence of inclusions of different species as that of the host minerals (e.g. muscovite in biotite), or the 'heterogeneous inclusions' (Figs. 3a-d; 4a, -c, -d; 5c; 6c; also see Gill, 2010), confirms that those inclusions did not originate from subgrains. Further, if the 'homogeneous inclusions' (host and inclusion of the same mineral species; e.g. Figs. 3c, -d; 4b; 5a, -b; -d; 6a, -b, -d) had formed by rotation of subgrains, those inclusions should have been sub-circular, and not parallelogram-shaped. Did the homogeneous- and the heterogeneous inclusions grow slowly in the matrix so as to be incorporated inside any adjacent faster growing mineral? If the host minerals were growing fast (such as the case in Fig. 1d), the inclusions would arrange haphazardly. Instead, the observed inclusions in many cases are oriented by maintaining a set of their boundaries roughly parallel to the cleavage planes of their host minerals. Many of those grains are parallelogram-shaped and are not rectangular. Secondly, even if any 'included' mica grains had come from the matrix, its undeformed shape is expected to be sub-circular (such as Fig. 1c; Passchier and Trouw 2005). On ductile shear, those 'included' grains are expected to

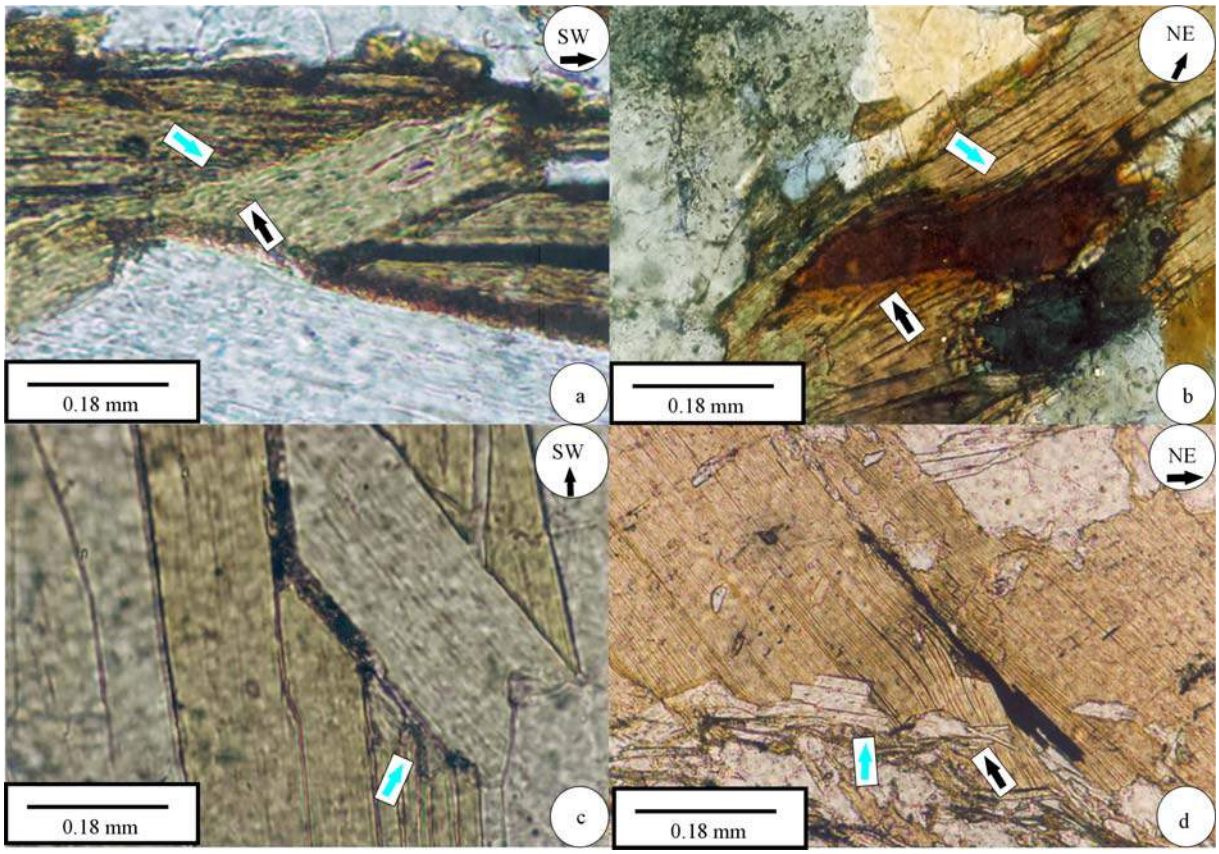

Fig. 6. All photos in plane polarized light.
(a, b), Sample: 12. Flanking microstructures. Biotite inclusions are sheared into parallelogram shapes. (a), The cleavage planes of the host are swerved at the margin of the inclusion (blue arrow). Internal deformation of the inclusion is inferred from its warped cleavage planes. A pair of margins of the inclusion roughly parallels the cleavage planes of the host, while the other pair is at ~25°. (b), Pronounced but local convex up (black arrow) and concave up (blue arrow) cleavage plane of the host mineral is noted near the margins of the inclusion. A pair of margins of the inclusion roughly parallels the cleavage planes of the host, while the other pair is at ~26°. Sample: 11. (c), Sample: 1. A muscovite included within biotites. Even though the inclusion is sheared into a parallelogram shape, the cleavage planes of the host mineral have remained straight. Only a part of the inclusion margin (blue arrow) is dynamically recrystallized. A pair of margins of the inclusion roughly parallels the cleavage planes of the host, while the other pair is at ~35°. (d), Sample: 4. Nearly rectangular muscovite inclusions in a stacked fashion (blue arrow) inside a biotite host. Over the kinked portion of the biotite grain, an irregular shaped muscovite grain nucleated (black arrow).

become sub-elliptical. Shearing of circular objects on shear commonly become elliptical (Davis and Reynolds 2007). On the contrary, most of the observed inclusions (Figs. 3a, -c, -d; 4a-d; 5a-d; 6a-c) are parallelograms, and a few are even trapezoid-shaped (Figs. 7a-c). Thus, those inclusions do not originate from the matrix.

The studied inclusions cannot be equated with peg structures (Wahlstrom, 1955) nor neocrystallization along dilation zones (Vernon, 1977). This is because most of them do not possess distinct lobate margins (Figs. 3-7). Thus, the inclusions are inferred to form from a different source of mineralization. Foliation planes that are planar on a regional to micro-scale (e.g. Fig. 3a; Mukherjee, 2010a, b; Mukherjee and Koyi, 2010a) indicate that an elongated inclusion arising from rock flexing, as proposed by Passchier and Trouw (2005), is not possible. The Sutlej section of the HHC do possess small-scale intrafolial folds (Mukherjee and Koyi 2010a), but no large scale folds exist. However, regional folds have been reported from the HHC along other river sections, such as from Bhutan (Carosi et al., 1999). When inclusions are seen inside mica host minerals (Figs. 3a-c but also others), no progressive variation in sizes of the inclusions are apparent. Statistical methods were not employed to study these variations. Unlike Vernon and Clarke (2008), variation in growth rate of the host micas and any increase in temperature of the bulk rock was not attempted.

The studied inclusions are distinct and most are disconnected with sharp straight margins (Figs. 3-7). They are therefore neither retrogressed products that were included at the margins (e.g. garnet to chlorite alteration) nor did they form in irregular channels inside the host minerals such as the ‘hour-glass structures’ or the ‘window structures’ developed in serpentinized olivine (Deer et al., 1992). The contacts between the original minerals and their retrogressed products, on the other hand, are rough (e.g. fig. 4.80 of Vernon, 2004). The margins of a number of inclusions are sharp and cannot be

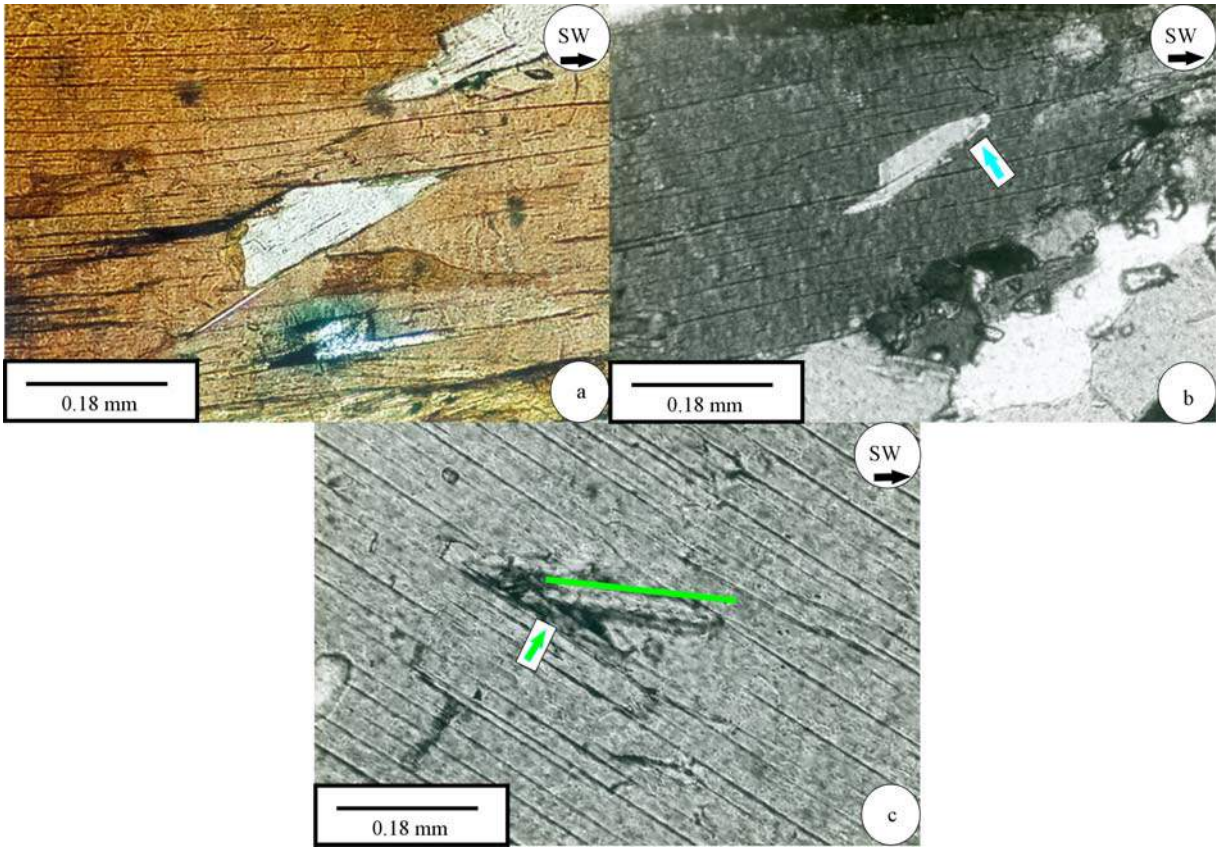

Fig. 7. (a–b) show trapezoid-shaped inclusion of biotite inside biotite host minerals. The cleavage planes of the trapezoid inclusions are at an angle with that of the host grain. Cleavage planes of the host grain are undeflected at their contacts with the inclusion. Cleavage planes of the trapezoids roughly parallel their longest margins. In Fig. 7a, the trapezoid margin has remained totally unaffected by dynamic recrystallization, whereas in Fig. 7b, dynamic recrystallization is noted (arrow). In Fig. 7a from sample: 8, the angle between the longest margin of the trapezoid and the cleavage planes of the host is ~30°. In Fig. 7b from sample: 16, the angle between the longest margin of the trapezoid and the cleavage planes of the host is ~32°. Fig. 7c. Sample: 13. An elongated inclusion of muscovite inside a host of muscovite grain shows some amount of breakage of the host mineral (arrow). Margin of the inclusion is curved, which indicates its internal deformation. A pair of margins of the inclusion roughly parallels the cleavage planes of the host, while the other pair is at ~33°. Fig. 7a is in plane polarized light and Figs. 7b-c in cross polarized light.

the products of any reaction or alteration. A few cases of diffuse margins do occur (Figs. 4a, -b, -d; 5b-d; 6a, -b), but those are related with a structural phenomenon that is discussed as 'flanking structures' (Passchier, 2001; Exner et al., 2004; Exner et al., 2006; Exner and Dabrowski, 2010). Thus, these inclusions are genetically not related to, nor were affected by, the M_3 retrograde metamorphism. For the same rationale, (i) amphibolite facies reaction between muscovite and Ca-amphibole giving rise to biotite (Deer et al., 1992) or reaction in biotite-, garnet-, staurolite-, kyanite- or sillimanite-zone where muscovite and biotite occur as reactants and/or products (Yardley, 1996) could not give rise to the studied inclusions. Because the studied shear zone rocks are at least 15 km NE to the 1866 ± 10 Ma old Wangtu Granite body (Singh et al., 1994; see Fig. 2), the latter's thermal effects (i.e. prior low-grade M_1 metamorphism) giving rise to micas and/or formation of their inclusions widespread in the shear zone is quite unlikely.

Formation of muscovite and biotite inclusions with a preferred orientation within biotite host mineral in the Broken hill region, Australia was explained by Vernon (1977) to be due to deformation and recrystallization of biotite under lower amphibolite facies condition. The Himalayan M_2 metamorphism and the concomitant D_2 deformation (Jain et al., 2002) also took place under similar condition of greenschist to amphibolite metamorphic facies. Thus, because no other genetic models fit, mica inclusions within micas (Figs. 3-7) appear to originate through local recrystallization of the host micas related to the M_2 (prograde) metamorphism simultaneous to the D_2 deformation. However, the limitation is that the present study could not specify the exact mechanism of recrystallization that led to the formation of one mica species from the other and its exact relation with the metamorphic phase.

Recrystallization devoid of any ambient stress leads to strain free grains (e.g. Vernon, 1977). Whereas, parallelogram geometry (Figs. 3b-d; 4a, -d; 5a; 6b) of some of the mica inclusions show a top-to-SW ductile shear (D_2-deformation phase), that match well with the other shear sense indicators in micro-scale as well as those in the field (Mukherjee, 2010a, b; Mukherjee and Koyi, 2010a). Therefore, these inclusions definitely formed by recrystallization, most possibly from the host minerals themselves when the future inclusions belonged to the same species, during (or before) the D_2-phase of deformation of top-to-SW ductile shear. A few (Fig. 4c), but not all (Figs. 3b-d; 4a, -d; 5a, -c; 6b, -c) parallelogram-shaped inclusions have pressure shadows as tails that roughly parallels the cleavage planes of the host minerals. This may indicate that the cleavage planes are the preferential sites of transport and precipitation of dissolved minerals, from the host minerals themselves in some cases, which now occur as inclusions. However, sharp and straight boundaries of inclusions indicate that after formation the inclusions were not affected by dissolution at margins. This is contrary to Simpson (1998) who documented rounded inclusions (here reproduced in Fig. 1e) from a shear zone at Parry sound domain gneiss, Ontario (also see Gower and Simpson, 1992).

Several $^{40}Ar/^{39}Ar$ dates of micas are available from the Himalaya (Najman et al., 1997; review by Pande 1999; Paudel and Arita 2006; Paudel 2011; Schlup et al., 2011), and other orogens (Dunlap et al., 1991; Zhu et al., 2005; Peng et al., 2006; Markley et al., 2007 and many others). Besides, Sanchez et al. (2011) dated by $^{40}Ar/^{39}Ar$ method newly formed micas, and Rolland et al. (2008) syn-kinematic micas. Kramar et al. (2001) discussed Ar-loss induced difficulty in dating micas. However, dates of inclusions of micas are not available to the knowledge of the author. Notice that the phrase 'inheritance of mineral grain' has been used to describe grains coming from a previous sedimentary rock. Such mineral grains are therefore completely different from inclusion of minerals within other minerals.

4 Conclusions

This study describes the morphologies of mica inclusions in mica host minerals from the Sutlej section of the Higher Himalayan Crystalline and selectively speculates on their genesis. The inclusions are possibly the products of the M_2 prograde metamorphic event, where some of the inclusions underwent a concomitant top-to-SW ductile shear of the Himalayan D_2 deformation leading to parallelogram shapes. The M_2 and the D_2 initiated from ~25 Ma. Tails roughly parallel to the cleavage planes of the host minerals suggesting movement of the pressure solution along the cleavage planes in a preferred direction along NE/SW direction related to top-to-SW shear. This probably is a micro-structural feature without any regional implication. Sharp boundaries of few inclusions indicate no dissolution after their formation. Mica inclusions grew in two directions: along and at high-angles to the cleavage planes in the host micas. The (001) cleavage planes of micas also are known to develop overgrowth, exsolution and topotactic intergrowths (Ferraris et al., 2001; Fleet et al., 2009). Deformation of an inclusion of the same species as that of the host mineral is likely to involve a negligible difference in viscosity between the two grains. Shearing of weaker inclusions of biotite within stronger muscovite is expected to result in parallelogram-shaped inclusions. Flanking microstructures defined by inclusions that cut across and deflect the cleavage planes of their host minerals reliably indicate a top-to-SW shear, whereas the observed trapezoid-shaped inclusions are a new observation.

The parallelogram-shaped inclusions are structurally anisotropic with their host minerals, and are interpreted not to originate from subgrains. The host minerals are neither pseudomorphs nor isomorphs of the inclusions. The preferred orientation of inclusions indicates that the inclusions were not incorporated from the matrix, and that the inclusions attempted to minimize their interfacial energies. Lack of variation in sizes of the inclusions from center to rim of the host grains makes it difficult to comment on any variation in temperature of the rocks and the growth rate of the host grains. Further, as the inclusions occur in rocks that were not folded, the genesis of the inclusions does not obviously correlate with folding. Their discrete geometries with sharp margins indicate that the inclusions were not products of nor affected by retrogression/alteration due to the Himalayan M_3 metamorphism. Lack of any visually decipherable pattern of inclusions such as linear or curvilinear/spiral inside the host mineral make these inclusions unfit to decipher ductile shear sense/tectonic movement directions. Unlike mica inclusions inside micas, quartz inclusions inside garnets were however noted in a different study from the same terrain and the shear sense was interpreted (e.g. Mukherjee and Koyi 2010a). Lastly, whether inclusions inherited from matrix or they grew syn-kinematically might get confirmed from a separate study of geochemistry/mineral chemistry.

Acknowledgements

The study was supported by Department of Science and Technology's (New Delhi) Grant: SR/FTP/ES-117/2009.

The two anonymous reviewers are thanked for constructive criticism. Previous reviews by Chris Talbot, Rodolfo Carosi, Tim Bell, David Rowley, Jonathan Imber, and Delores Robinson were helpful.

Manuscript received Dec. 12, 2013,
May 20, 2014
edited by Liu Xinzhu and Fei Hongcai

References

Bell, T.H., 1978. Syntectonic nucleation of new grains in deformed mica. *Tectonophysics*, 51: T31–T37.

Bell, T.H., and Hobbs, B.E., 2010. Foliations and shear sense: A modern approach to an old problem. *J. Geol. Soc. India*, 75: 137–151.

Burchfiel, B.C., Chen, Z., Hodges, K.V., Liu, Y., Royden, L.H., Deng, C., and Xu, J., 1992. The South Tibetan Detachment System, Himalayan orogen: extension contemporaneous with and parallel to shortening in a collisional mountain belt. *Geol. Soc. Am. Special Paper*, 269: 1–41.

Carosi, R., Lombardo, B., Molli, G., Musumeci, G., and Pertusati, P.C., 1998. The South Tibetan detachment system in the Rongbuk valley, Everest region. Deformation features and geological implications. *J. Asian Earth Sci.*, 16: 299–311.

Carosi, R., Lombardo, B., Musumeci, G., and Pertusati, P., 1999, Geology of the Higher Himalayan Crystallines in Khumbu Himal (Eastern Nepal). *J. Asian Earth Sci.*, 17: 785–803.

Chambers, J., Caddick, M., Argles, T., Horstwood, M., Sherlock, S., Harris, N., Parrish, R., and Ahmad, T., 2009. Empirical constraints on extrusion mechanisms from the upper margin of an exhumed high-grade orogenic core, Sutlej valley, NW India. *Tectonophysics*, 477: 77–92.

Chambers, J., Parrish, R., Argles, T., Harris, N., and Horstwood, M., 2011. A short duration pulse of ductile normal shear on the outer South Tibetan detachment in Bhutan: alternating channel flow and critical taper mechanics of the eastern Himalaya. *Tectonics,* 30: TC2005.

Dai, S., Zhang, M.Z., Peng D.X., Wang, H.W., Wu, M.X., Chen, R.L., and Zhang, X., 2014. Tectonic and environmental evolutions of the Northern Tibetan Plateau prior to the collision of India with Asia. *Acta Geologica Sinica* (English Edition), 88(2): 425–443.

Davis, G.H., and Reynolds, S.J., 2007. Structural Geology of Rocks and Regions (second edition). New york: Wiley, 200.

Deer, W.A., Howie, R.A., and Zussman, J., 1992. An Introduction to the Rock-Forming Minerals. ELBS, 306, 350.

Dunlap, W.J., Teyssier, C., McDougallm, I., and Baldwin, S., 1991. Ages of deformation from K/Ar and $^{40}Ar/^{39}Ar$ dating of white micas. *Geology*, 19: 1213–1216.

Exner, U., and Dabrowski, M., 2010. Monoclinic and triclinic 3D flanking structures around elliptical cracks. *J. Structural Geol.*, 32: 2009–2021.

Exner, U., Grasemann, B., and Mancktelow, N.S., 2006. Multiple faults in ductile simple shear: analogue modeling of flanking structure systems. In: Buiter, S.J.H., and Schreurs, G. (eds), *Analogue and Numerical Modelling of Crustal-Scale Processes.* London: Geological Society (special publication), 253: 381–395.

Exner, U., Mancktelow, N.S., and Grasemann, B., 2004. Progressive development of s-type flanking folds in simple shear. *J. Structural Geol.*, 26: 2191–2201.

Faryad, S.W., Naholdikova, R., and Dolejš, D., 2010. Incipient eclogite facies metamorphism in the Moldenubian granulites revealed by mineral inclusions in garnet. *Lithos*, 114: 54–69.

Ferraris, C., Grobety, B., and Wessicken, R., 2001. Phlogopite exsolutions within muscovite: a first evidence for a higher temperature re-equilibration, studied by HRTEM and AEM techniques. *European J. Mineral.*, 13: 15–26.

Fleet, M.E., Deer, W.A., Howie, R.A., and Zussmann, J., 2009. *An Introduction to the Rock-Forming Minerals: Micas*. Vol 3 (second edition), ELBS, 211–213.

Fossen, H., 2010. *Structural Geology*. Cambridge: Cambridge University Press, 214, 215.

Godin, L., Grujic, D., Law, R.D., and Searle, M.P., 2006. Channel flow, extrusion and exhumation in continental collision zones: an introduction. In: Law RD, Searle MP (eds) Channel flow, extrusion and exhumation in continental collision zones 268. London: Geological Society (special publication), 1–23.

Gower, R.J.W., and Simpson, C., 1992. Phase boundary mobility in naturally deformed, high grade quartzofeldspathic rocks: evidence for diffusional creep. *J. Structural Geol.*, 14: 301–313.

Grasemann, B., Fritz, H., and Vannay, J.-C., 1999. Quantitative kinematic flow analysis from the Main Central Thrust Zone (NW-Himalaya, India): implications for a decelerating strain path and extrusion of orogenic wedges. *J. Structural Geol.*, l21: 837–853.

Heinrich, E.W.M., 1956. *Microscopic Petrography*. New York: McGraw-Hill Book Company, 28.

Gill, R., 2010. Igneous rocks and processes: a practical guide. Chichester: Wiley-Blackwell, 214–215, 371.

Guillot, S., and Replumaz, A., 2013. Importance of continental subductions for the growth of the Tibetan plateau. *Bull de la Société Géol de France*, 184: 199–223.

Hammer, J.E., Sharp, T.G., and Wessel, P., 2010, Heterogeneous nucleation and epitaxial crystal growth of magmatic minerals. *Geology*, 38: 367–370.

Jain, A.K., Kumar, D., Singh, S., Kumar, A., and Lal, A., 2000. Timing, quantification and tectonic modelling of Pliocene-Quaternary movements in the NW Himalaya: evidences from fission track dating. *Earth Planet. Sci. Lett.*, 179: 437–451.

Jain, A.K., Singh, S., and Manickavasagam, R.M., 2002. Himalayan Collision Tectonics. *Gondwana Research Group Memoir Number 7*. Hashimoto: Field Science Publishers, 33, 34.

Jain, A.K., Singh, S., Sushmita, Seth, P., and Shreshtha, M., 2012. Structurally controlled melt formation and accumulation: Evidence for channel flow in the Himalaya. Abstract in 27th Himalaya-Karakoram-Tibet Workshop (HKT). *J. Nepal Geol. Soc.*, 45: 2.

Janda, C., Hager, C., Grasemann, B., Draganits, E., Vannay, J-C., Bookhagen, B., and Thiede, R., 2002. The Karcham Normal Fault—implications for an active extruding wedge, Sutlej valley, NW Himalaya. *J Asian Earth Sci.*, 20:19–20.

Kelley, S.P., Bartlett, J.M., and Harris, N.B.W., 1997. Pre-metamorphic Ar-Ar ages from biotite inclusions in garnet. *Geochim. Cosmochim. Acta*, 61: 3873–3878.

Kohn, M.J., Wieland, M.S., Parkinson, C.D., and Upreti, B., 2005. Five generations of monazite in Langtang gneisses:

implications for chronology of the Himalayan metamorphic core. *J. Metamorphic Geol.*, 23: 399–406.

Kramar, N., Cosca, M.A., and Hunziker, J.C., 2001. Heterogeneous ^{40}Ar* distributions in naturally deformed muscovite: in situ UV-laser ablation evidence for microstructurally controlled intragrain diffusion. *Earth Planet. Sci. Lett.*, 192: 377–388.

Kretz, R., 1966. Interpretation of the Shape of Mineral Grains in Metamorphic Rocks. *J. Petrol.*, 7: 68–94.

Krol, M.A., Muller, P.D., and Idleman, B.D., 1999. Late Paleozoic deformation within the Pleasant Grove Shear Zone, Maryland: Results from ^{40}Ar/^{39}Ar dating of white mica. In: Valentino, D.W., and Gates, A.E. (eds), *The Mid-Atlantic Piedmont: Tectonic Missing Link of the Appalachians*. *Geol. Soc. Am. Special Paper*, 330: 93–112.

Law, R., Stahr, III D.W., Francsis, M.K., Ashley, K.T., Grasemann, B., and Ahmad, T., 2013. Deformation Temperatures and Flow Vorticities Near the Base of the Greater Himalayan Crystalline Sequence, Sutlej Valley and Shimla Klippe, NW India. *J. Struct. Geol.,* 54: 21–53.

Liu, J., Ye, K., Maruyama, S., Cong, B., and Fan, H., 2001. Mineral inclusions in Zircon from Gneisses in the Ultrahigh-Pressure Zone of the Dabie Mountains, China. *J. Geol.*, 109: 523–535.

Markley, M.J., Teyssier, C., and Cosca, M., 2002. The relation between grain size and ^{40}Ar/^{39}Ar date for Alpine white mica from the Siviez-Mischabel Nappe, Switzerland. *J. Structural Geol.*, 24: 1937–1955.

Morton, A.C., and Hallsworth, C., 1994. Identifying provenance-specific features of detrital heavy mineral assemblages in sandstones. *Sedimentary Geol.*, 90: 241–256.

Mukherjee, S., 2008. Manifestation of brittle thrusting in micro-scale in terms of micro-duplexes of minerals in the Higher Himalayan Shear Zone, Sutlej and Zanskar section, northwest Indian Himalaya. GeoMod2008. International Geological Modelling Conference. Florence, Italy. 22–24 September. Bolletino di Geofisica Teorica e Applicata, 49: 254–257.

Mukherjee, S., 2009. Ductile shearing of mineral grains nucleated in a host mineral of same species. *Geology Today*, 25: 52.

Mukherjee, S., 2010a. Structures at Meso- and Micro-scales in the Sutlej section of the Higher Himalayan Shear Zone in Himalaya. *e-Terra*, 7: 1–27.

Mukherjee, S., 2010b. Microstructures of the Zanskar Shear Zone. *Earth Sci. India*, 3: 9–27.

Mukherjee, S., 2011a. Mineral fish: their morphological classification, usefulness as shear sense indicators and genesis. *Intl. J. Earth Sci*., 100: 1303–1314.

Mukherjee, S., 2011b. Flanking Microstructures from the Zanskar Shear Zone, NW Indian Himalaya. *YES Network Bull.*, 1: 21–29.

Mukherjee, S., 2012. Tectonic implications and morphology of trapezoidal mica grains from the Sutlej section of the Higher Himalayan Shear Zone, Indian Himalaya. *J. Geol.*, 120: 575–590.

Mukherjee, S., 2013a. Higher Himalaya in the Bhagirathi section (NW Himalaya, India) — its structures, backthrusts, and extrusion mechanism by both channel flow and critical taper mechanisms. *Intl. J. Earth Sci.*, 102: 1851–1870.

Mukherjee, S., 2013b. Channel flow extrusion model to constrain dynamic viscosity and Prandtl number of the Higher Himalayan Shear Zone. *Intl. J. Earth Sci.*, 102: 1811–1835.

Mukherjee, S., 2013c. Atlas of Shear Zone Structures in Meso-scale. Cham: Springer.

Mukherjee, S., 2013d. *Deformation Microstructures in Rocks*. Berlin: Springer, 1–111.

Mukherjee, S., and Biswas, R., 2014. Kinematics of horizontal simple shear zones of concentric arcs (Taylor–Couette flow) with incompressible Newtonian rheology. *Intl. J. Earth Sci.*, 103: 597–602.

Mukherjee, S., and Koyi, H.A., 2009. Flanking Microstructures. *Geol. Magazine*, 146: 517–526.

Mukherjee, S., and Koyi, H.A., 2010a. Higher Himalayan Shear Zone, Sutlej section: structural geology and extrusion mechanism by various combinations of simple shear, pure shear and channel flow in shifting modes. *Intl. J. Earth Sci.*, 99: 1267–1303.

Mukherjee, S., and Koyi, H.A., 2010b. Higher Himalayan Shear Zone, Zanskar Indian Himalaya—microstructural studies and extrusion mechanism by a combination of simple shear and channel flow. *Intl. J. Earth Sci.*, 99: 1083–1110.

Mukherjee, S., Koyi, H.A., and Talbot, C.J., 2012. Implications of channel flow analogue models for extrusion of the Higher Himalayan Shear Zone with special reference to the out-of-sequence thrusting. *Intl. J. Earth Sci.*, 101: 253–272.

Najman, Y.M.R., Pringle, M.S., Johnson, M.R.W., Robertson, A.H.F., and Wijbrans, J.R., 1997. Laser ^{40}Ar/^{39}Ar dating of single detrital muscovite grains from early foreland-basin sedimentary deposits in India: Implications for early Himalayan evolution. *Geology*, 25: 535–538.

Pande, K., 1999. Present status of K-Ar and ^{40}Ar-^{39}Ar date from the Himalaya. In: Jain, A.K., and Manickavasagam, R.M. (eds), *Geodynamics of the NW Himalaya*. Gondwana Research Group Memoir, 6, Osaka, 237–244.

Passchier, C.W., 2001. Flanking Structures. *J. Structural Geol.*, 23: 951–962.

Passchier, C.W., and Trouw, R.A.J., 2005. *Microtectonics*. Berlin: Springer-Verlag, 139, 191, 207, 208.

Paudel, L.P., 2011. K-Ar Dating of White Mica from the Lesser Himalaya, Tansen-Pokhara Section, Central Nepal: Implications for the Timing of Metamorphism. *Nepal J. Sci. Technol.*, 12: 242–251.

Paudel, L.P., and Arita, K., 2006. Thermal evolution of the Lesser Himalaya, central Nepal: Insights from K-white micas compositional variation. *Gondwana Research*, 9: 409–425.

Peng, J., Zhou, M-F., Hu, R., Shen, N., Yuan, S., Bi, X., Du, A., and Qu, W., 2006. Precise molybdenite Re–Os and mica Ar-Ar dating of the Mesozoic Yaogangxian tungsten deposit, central Nanling district, South China. *Miner Deposita*, 41: 661–669.

Phillips, D., and Miller, J.M., 2006. ^{40}Ar/^{39}Ar dating of mica-bearing pyrite from thermally overprinted Archean gold deposits. *Geology*, 34: 397–400.

Philpotts, A.R., and Ague, J.J., 2009. Principles of Igneous and Metamorphic Petrology (second edition). Cambridge: Cambridge University Press, 292.

Richards, A., Argles, T., Harris, N., Parrish, R., Ahmad, T., Darbyshire, F., and Draganits, E., 2005. Himalayan architecture constrained by isotopic tracers from clastic sediments. *Earth Planet. Sci. Lett.*, 236: 773–796.

Rolland, Y., Rossi, M., Cox, S.F., Corsini, M., Mancktelow, N., Pennachhioni, G., Fornari, M., and Boullier, A.M., 2008.

$^{40}Ar/^{39}Ar$ dating of synkinematic white mica: insights from fluid-rock reaction in low-grade shear zones (Mont Blanc Massif) and constraints on timing of deformation in the NW external Alps. In: Wibberley, C.A.J., Kurz, W., Imber, J., Holdsworth, R.E., and Collettini, C. (eds.), *The Internal Structures of Fault Zones: Implications for Mechanical and Fluid Flow Properties*. Geological Society, London, Special Volume, 299: 293315.

Roycroft, P., 1991. Magmatically zoned muscovite from the peraluminous two-mica granites of the Leinster batholith, southeast Ireland. *Geology*, 19: 437–440.

Sanchez, G., Rolland, Y., Schneider, J., Corsini, M., Oliot, E., Goncalves, P., Verati, C., Lardeaux, J-M., and Marquer, E., 2011. Dating low-temperature deformation by $^{40}Ar/^{39}Ar$ on white mica, insights from the Argentera-Mercantour Massif (SW Alps). *Lithos*, 125: 521–536.

Schlup, M., Steck, A., Cater, A., Cosca, M., Epard, J-L., and Hunziker, J., 2011. Exhumation history of the NW Indian Himalaya revealed by fission track and $^{40}Ar/^{39}Ar$ ages. *J. Asian Earth Sci.*, 40: 334–350.

Searle, M.P., Law, R.D., Godin, L., Larson, K.P., Streule, M.J., Cottle, J.M., and Jessup, M.J., 2008. Defining the Main Central Thrust in Nepal. *J. Geol. Soc.*, 165: 523–534.

Simpson, C., 1998. High-temperature Grain-Boundary and Phase Boundary Migration. In: Snoke, AW, Tullis J, and Todd, V.R. (eds), *Fault-related Rocks A Photographic Atlas*. Princeton: Princeton University Press, 270.

Singh, S., Claesson, S., Jain, A.K., Sjoberg, H., and Gee, D.G., 1994. Geochemistry of the Proterozoic peraluminous granitoids from the Higher Himalayan Crystalline (HHC) and Jutogh Nappe, NW Himalaya, Himachal Pradesh, India. *J. Nepal Geol. Soc*., 10.

Srikantia, S.V., and Bhargava, O.N., 1998. Geology of Himachal Pradesh. *Geol. Soc. Ind., Bangalore*, 1–406.

Takagi, H., Arita, K., Sawaguchi, T., Kobayashi, K., and Awaji, D., 2003. Kinematic history of the Main Central Thrust zone in the Langtang area, Nepal. *Tectonophysics*, 366: 151–163.

Vannay, J.-C., and Grasemann, B., 2001. Himalayan inverted metamorphism and syn-convergence extension as a consequence of a general shear extrusion. *Geol. Magazine*, 138: 253–276.

Vannay, J.-C., Grasemann, B., Rahn, M., Carter, A., Baudraz, V., and Cosca, M., 2004. Miocene to Holocene exhumation of metamorphic crustal wedge in the NW Himalaya: Evidence for tectonic extrusion coupled to fluvial erosion. *Tectonics*, 23 (TC1014): 1–24.

Vannay, J.-C., Sharp, D.Z., and Grasemann, B., 1999. Himalayan inverted metamorphism constrained by oxygen thermometry. *Contribu. Mineral. Petrol.*, 137: 90–101.

Vernon, R.H., 1977. Microfabric of mica aggregates in partly recrystallized biotite. *Contribu. Mineral. Petrol*., 61: 175–185.

Vernon, R.H., 2004. *A Practical Guide to Rock Microstructure*. Cambridge: Cambridge University Press, 102, 105, 106, 190–191, 209, 210, 289, 410, 445.

Vernon, R.H., and Clarke, G., 2008. *Principles of Metamorphic Petrology*. Cambridge: Cambridge University Press, 74, 76, 86, 88.

Wahlstrom, E.E., 1955, Petrographic Mineralogy. New York: John Wiley & Sons, 29, 30.

Wu, Z.H, Yang, Y., Barosh, P.J., Wu, Z.H., and Zhang, Y.L., 2014. Tectonics and topography of the Tibetan Plateau in Early Miocene. *Acta Geologica Sinica* (English Edition), 88 (2): 410–424.

Wilson, C.J.L., and Bell, I.A., 1979. Deformation of biotite and muscovite: optical microstructure. *Tectonophysics*, 58: 179–200.

Yardley, B.W., 1996. *An Introduction to Metamorphic Petrology*. Longman Earth Science Series. Harlow: Prentice Hall, 112.

Yin, A., 2006. Cenozoic tectonic evolution of the Himalayan orogen as constrained by along-strike variation of structural geometry, extrusion history, and foreland sedimentation. *Earth-Sci. Rev.*, 76: 1–131.

Zhu, G., Wang, Y., Liu, G., Niu, M., Xie, C., and Li, C., 2005. $^{40}Ar/^{39}Ar$ dating of strike-slip motion on the Tan–Lu fault zone, East China. *J. Structural Geol.*, 27: 1379–1398.

About the first author

Soumyajit MUKHERJEE, Faculty at Indian Institute of Technology Bombay, India. Associate Editor of International Journal of Earth Sciences. Received 'Hutchison Young Scientist Award' from International Union of Geological Sciences (IUGS).